Title
Combined effects of drebrin A and mDia2 formin on actin nucleation, elongation, and bundling

Author
Ginosyan, Anush Aram

Publication Date
2017

Peer reviewed|Thesis/dissertation

UNIVERSITY OF CALIFORNIA

Los Angeles

Combined effects of drebrin A and mDia2 formin on actin nucleation, elongation, and bundling

A thesis submitted in partial satisfaction
of the requirements for the degree Masters of Science
in Biochemistry, Molecular and Structural Biology

by

Anush Aram Ginosyan

2017

ABSTRACT OF THE THESIS

Combined effects of drebrin A and mDia2 formin
on actin nucleation, elongation, and bundling

by

Anush Aram Ginosyan

Master of Science in Biochemistry, Molecular and Structural Biology
University of California, Los Angeles, 2017

Professor Emil Reisler, Chair

Actin cytoskeleton is important for neuronal morphology and function. Many accessory proteins, including brain-specific drebrin A and diaphanous family of formins (mDia), regulate actin dynamics in neuronal substructures, such as dendritic spines. In order to probe for possible interrelation of drebrin and mDia2 formin, we examined their combined effects on actin polymerization, bundling, and binding. We identified drebrin A as a new interacting partner of mDia2 formin. Our results suggest two sites of interaction between drebrin A and mDia2, with the C-terminal region of drebrin binding to formin's FH2 domain and the "actin binding core" of drebrin binding to formin's C-terminal "tails." We found that drebrin A inhibits mDia2-driven actin nucleation without affecting the rate of its processive elongation. Drebrin also abolishes actin bundling mediated by FH2 domain of mDia2. Thus, our data contribute to the mechanistic understanding of actin regulation and its role in neuronal function and development.

The thesis of Anush Aram Ginosyan is approved.

Margot Elizabeth Quinlan

Joseph Ambrose Loo

Emil Reisler, Committee Chair

University of California, Los Angeles

2017

Table of Contents

Introduction

In the central nervous system, chemical synapses are the major form of communication between pre- and post- synaptic neurons [1]. These synapses are plastic and undergo modification during development. On the post-synaptic side, small actin rich protrusions on neuronal dendrites, known as dendritic spines, are important for receiving chemical signals from a pre-synaptic axon and transmitting them to the neuron's cell body [1]. Mature dendritic spines commonly have a bulbous head and are connected to the dendrite via a thin neck. This type of dendritic spine is referred to as mushroom shaped; however, there are numerous classes of spine shapes including thin, stubby, and cup [2] (Fig.1). Live imaging studies have revealed that dendritic spines are dynamic structures that can change in size and shape [3]. The size of the spine's head is correlated with the strength of synaptic transmission [4]. Thus, spine morphology and function are directly linked. It is known that changes in spine morphology play a role in higher brain functions such as learning and memory [5].

Actin cytoskeleton regulates the development and morphology of dendritic spines, and is important for synaptic plasticity [5, 6]. Both monomeric (G-actin) and filamentous (F-actin) actin are present in dendritic spines. The dendritic spine head consists of mainly branched filamentous actin, whereas the dendritic spine neck is composed of bundled actin filaments [7]. It has been suggested that the dendritic spine head contains two pools of F-actin: a stable pool and a dynamic pool [8]. The stable F-actin pool exhibits a slower treadmilling rate relative to the dynamic pool. Moreover, the stable F-actin pool is found at the base of the spine head, whereas the dynamic pool is located at the spine head periphery. It is likely that the stable and dynamic pools of F-actin play distinct roles in the shape regulation of dendritic spine [8].

F-actin is regulated by many accessory proteins. These actin binding proteins perform a wide range of functions, including F-actin nucleation, side binding, bundling, cross-linking, capping, severing, and depolymerization. Thus, these proteins are critical for the formation and dynamics of the actin cytoskeleton in dendritic spines [9, 10].

Drebrin is one of the key actin regulators in dendritic spines [6, 11–13]. Drebrin's loss is reportedly associated with impaired higher order brain functions and occurs in Alzheimer's disease, Down syndrome and epilepsy patients [12, 14, 15]. Three drebrin isoforms are known, drebrin A (adult isoform), drebrin sA (small adult isoform), and drebrin E (embryonic isoform) [6, 16]. Drebrin A is specifically enriched in dendritic spines, whereas drebrin E is ubiquitous [6, 11]. It was shown that drebrin A inhibits F-actin depolymerization from both barbed and pointed ends, effectively stabilizing actin filaments [17]. Furthermore, the stable actin pool in dendritic spines consists of drebrin-decorated F-actin [6, 11]. It was also shown that spine head size correlates with drebrin A content in dendritic spines [18]. Thus, drebrin A is an actin binding protein that regulates actin dynamics in dendritic spines, thereby affecting dendritic spine morphology.

Formins recently emerged as an important class of neuronal regulators. The 15 distinct mammalian formins known have been classified into 7 subfamilies through phylogenetic analysis: DAAM, Delphilin, Dia, FHOD, FMN, FMNL, and INF (see Ref [19] for review). Formins are both actin nucleators and processive elongating factors that promote the formation of actin filaments [19]. Accumulating evidence suggests that formins play a role in neuronal function and development [20–23]. It has been shown that mammalian formin mDia2 expresses in neurons and localizes to the tips of dendritic filopodia [20, 24, 25]. mDia2 expression increases during the development of filopodia into dendritic spines [20]. Additionally, silencing mDia2 expression by RNAi results in a decreased number of dendritic filopodia and an increased number of small, stubby spines [20]. Thus, mDia2 formin can potentially be a regulator of actin nucleation and polymerization in dendritic spines. However, its interrelations with other neuronal regulators are yet to be elucidated.

Formins, in their functional form, are antiparallel dimers [19]. All formins, including mDia2, have adjacent FH1-FH2 domains. In cells, free globular actin (G-actin) is mostly complexed with profilin. Formin-assisted actin polymerization accelerates dramatically in the

presence of profilin-actin compared to actin alone. This effect is due to the presence of poly-proline motifs within FH1 domains of formins. Poly-proline rich motifs serve as “traps” for profilin-actin complexes increasing the local concentration of actin monomers near the barbed end. Thus, under physiological conditions, formins processively move with growing barbed ends of actin filaments and assist filament elongation through FH1 dependent profilin-G-actin transfer. FH2 domain of mDia2 is a homodimer. It is necessary and sufficient for actin nucleation and bundling. In addition, it was documented that formin’s C-terminal extensions (“tails”), downstream of FH2 domain, also aid actin nucleation (FH2-C > FH2). C-terminal “tail” truncations in formin decrease the duration of processive runs in the presence of profilin-actin (the amount of time formin resides on the barbed end of actin filaments) [26].

Prior work done in Emil Reisler’s lab showed that barbed end actin elongation is inhibited in the presence of drebrin A (unpublished). Because both drebrin A and mDia2 formin affect F-actin’s barbed ends, we hypothesize that they may interact directly or influence each other’s activities. We chose to study mDia2 formin because it was shown that mDia2 expresses in filopodia prior to dendritic spine formation [20].

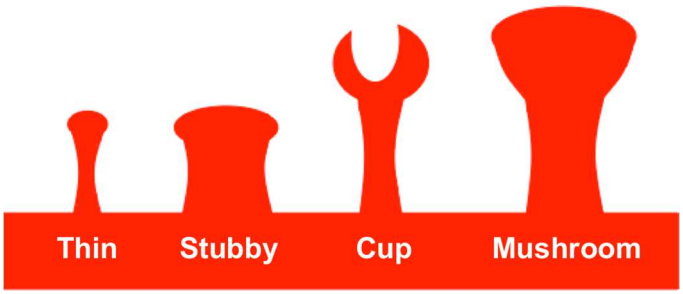

FIGURE1: **Schematic representation of mature dendritic spine morphologies.** Dendritic spines display a wide range of morphologies. They can be classified into the four categories shown above: thin, stubby, cup, and mushroom. Mushroom shaped spines, with a bulbous head supported by a thin neck, are most common.

Results

Choice of recombinant drebrin A and mDia2 formin constructs. Our goal was to assess the combined effects of mDia2 formin and drebrin A on actin polymerization, bundling, and binding in order to probe for possible interrelation between these two actin regulators. For this study we employed N- and C- terminal truncations of mDia2 formin (FH1-FH2-tail (**FFC**), FH1-FH2 (**FF**), FH2, and C-terminal "tail" constructs (Fig.2a and 2b)). We did not test full length (FL) mDia2 because (as most formins) it is autoinhibited *in vitro* [19]. This inhibition allows for tight regulation of formin's activity *in vivo* and is released in response to cellular signaling. In the autoinhibited conformation, the DID domain of mDia2 (located in N-terminal part of the protein) tightly binds to its DAD domain (located in its C-terminal "tail" region). Such interaction strongly suppresses formin's ability to nucleate and elongate actin filaments [19]. Thus, in all mDia2 constructs employed, the N-terminal part of the protein was truncated to make them constitutively active in actin polymerization (Fig.2b). The C-terminal "tail" region of most formins is involved in their autoinhibition and is also known to be a "hot spot" for binding of regulatory proteins and microtubules [19, 26–29]. Thus, for this study we created a FF formin construct lacking the C-terminal "tail" to test if any effects of drebrin A are mediated through its interference with this region of mDia2.

In this work we employed full length drebrin A (DrbFL) and several of its C-terminal truncated constructs. Sequence 1-300 of drebrin (Drb1-300) is its "actin-binding core," which contains three different domains implicated in F-actin binding [17, 30] (Fig.2c). The rest of drebrin A is predicted to be intrinsically disordered (Fig. 2d). Full length drebrin and Drb1-300 construct have similar affinities to F-actin but different binding stoichiometries [30, 31], suggesting that Drb1-300 makes the main contribution to drebrin's interaction with actin filaments. Potentially, drebrin A may regulate mDia2 via (1) direct interaction or (2) indirectly, by changing the structure and dynamics of actin filaments and/or interfering with formin's binding site(s) on actin. The drebrin A construct containing only the "actin binding core" region (Drb1-

300) may help to distinguish between these two possibilities. For instance, if DrbFL but not Drb1-300 affects mDia2-driven actin polymerization and/or remodeling, then drebrin's effect(s) are unlikely to be mediated through actin. Thus, in our assays we compared full lenghth drebrin and Drb1-300 construct ("actin-binding core"). We used Drb2-252 construct in some of the experiments in attempt to clarify the domain requirements for the observed effects (Fig.2d).

Drebrin inhibits mDia2 formin-driven actin nucleation. To examine the effect of drebrin A on mDia2-driven actin nucleation and elongation we employed total internal reflection fluorescent microscopy (TIRFM). To determine if full length drebrin A affects mDia2-FFC-driven actin nucleation, we polymerized Alexa488-SE-labeled G-actin with mDia2-FFC in the absence and presence of DrbFL. After 10 min we stopped the reactions and imaged the resulting products on polyK coated slide surfaces. The number of filaments formed indicates the efficiency of actin nucleation in the reaction. We saw a dramatic decrease in number of actin filaments nucleated by mDia2-FFC within 10 minutes when drebrin was present, compared to mDia2-FFC alone (Fig.3a). Thus, we concluded that drebrin A inhibits actin nucleation by mDia2-FFC.

Next, we employed time lapse TIRFM to determine the rates of mDia2-FFC driven elongation of individual actin filaments in the presence and absence of DrbFL. In these assays we used 1:5 molar ratio of actin to human profilin-1 to ensure that majority of actin monomers are complexed with profilin. Profilin-actin monomers can bind to the FH1 domain of mDia2-FFC and support processive elongation. We found that DrbFL does not affect the rates of actin elongation by mDia2-FFC (Fig.3b). The rate of actin subunit addition to the barbed ends did not change when drebrin was present (14.1+/-2.9 subunits/s, n=24 filaments), compared to mDia2-FFC alone (14.5+/-3.1 subunits/s, n=21 filament). Thus, while drebrin A inhibits actin nucleation by mDia2 formin, filament elongation rate is not affected. It is worth mentioning, that unpublished work done in our lab (Grintsevich EE, unpublished) indicated that while the rate of

actin elongation driven by mDia2-FFC is not changed in the presence of drebrin A, formin's processivity (time that formin resides on the barbed end of filament) is reduced.

Domain requirements for drebrin's inhibition of mDia2-driven actin polymerization. To gain mechanistic understanding of the overall effect of drebrin on mDia2-driven actin polymerization we employed pyrene fluorescence assays and truncated constructs of both proteins. Increase in pyrene fluorescence signal upon actin polymerization is a convenient tool used in bulk solution assays. It reports on overall actin polymerization, including actin nucleation and elongation.

First, we tested the effect of different DrbFL concentrations, ranging from sub-saturating to saturating levels, on actin polymerization driven by mDia2-FFC. We found that the inhibitory effect of DrbFL was concentration dependent: as drebrin concentration increased relative to formin concentration the rate of actin polymerization decreased (Fig.4a). Moreover, the lag phase at the onset of actin polymerization, which is generally attributed to actin nucleation, becomes longer as drebrin concentration increases. We calculated the drebrin concentration necessary to achieve half the maximum inhibition of actin polymerization to be 0.04uM DrbFL (Fig.4b). This concentration of DrbFL is significantly lower than that required to saturate 1 uM of actin (based on the Kd~50nM and 5:1 actin:DrbFL binding stoichiometry) but close to mDia2-FFC concentration in the reaction (30 nM). This suggests that drebrin may inhibit mDia2 via direct interaction. The same inhibitory effect of DrbFL was observed both with and without profilin (Fig.4c and 4d). Thus, results of our pyrene fluorescence assays (Fig.4) are consistent with our TIRFM data showing drebrin's inhibition of actin nucleation by mDia2 formin (Fig.3a).

In order to identify the region(s) of drebrin A responsible for its inhibition of mDia2 formin-driven actin polymerization, we employed Drb1-300 and Drb2-252 constructs. Like full-length drebrin, the inhibitory effect of Drb1-300 and Drb2-252 constructs was concentration dependent: as their concentration increased relative to formin concentration the rate of actin polymerization decreased (Fig.5a and Fig.6a). However, the concentration of Drb1-300 and

Drb2-252 necessary to achieve half maximum inhibition of actin polymerization were 0.81uM and 2.0 uM, respectively (Fig.5b and 6b). Thus, mDia2-FFC inhibition by Drb1-300 and Drb2-252 was much weaker than that of DrbFL (40 nM). This suggested two possibilities: (1) drebrin has two independent mDia2 binding sites or (2) truncating the drebrin molecule after residue 300 disrupts its mDia2 binding site. These possibilities were examined by considering the mDia2 regions affected by drebrin.

We set out to identify mDia2 region(s) affected by drebrin using mDia2-FFC and mDia2-FF constructs in pyrene florescence assays (Fig.7). Actin polymerization driven by mDia2-FFC formin in the presence and in the absence of profilin is inhibited by full-length drebrin A. This inhibition is reduced but not abolished by drebrin's "actin-binding core" (Drb1-300) (Fig.7a and 7c). For comparison, we examined the effect of drebrin A on actin polymerization driven by mDia2 FH1-FH2 construct (mDia2 FF), which is missing the C-terminal "tails". These mDia2-"tails" are shown to aid formin-driven actin nucleation and processivity [26, 32]. Interestingly, actin polymerization driven by mDia2-FF (both in the presence and absence of profilin) is partially inhibited by full-length drebrin but not by Drb1-300 (Fig.7b and 7d). Based on Drb1-300 inhibition of mDia2-FFC but not mDia2-FF, we hypothesized that C-terminal "tails" of mDia2 may interact with "actin-binding core" of drebrin (Drb1-300). Moreover, the observed inhibition of both, mDia2-FFC and FF by DrbFL, indicate that the C-terminal region of drebrin (residues 301-706) may directly interact with the FH1-FH2 region of mDia2 formin. Thus, the results of our pyrene florescence assays suggest that drebrin A may have two different mDia2 interaction sites (Fig.8).

Drebrin A is a new interacting partner of mDia2 formin. Next, we tested for direct interactions between drebrin A and mDia2 formin in pull-down assays. Our pyrene florescence assays suggested that drebrin interacts with mDia2 C-terminal "tail" regions. In order to test this directly, we performed a pull-down assay in which immobilized GST fused mDia2 C-terminal "tails" were incubated with full-length drebrin (Fig.9). We were able to pull down full-length

drebrin with the C-terminal of mDia2 but not with GST. Visual inspection indicates that we pulled a sub-stoichiometric amount of full-length drebrin, which is indicative of a low affinity interaction. Thus, our pull-down revealed direct, albeit weak binding between mDia2 C-terminal “tails” and full-length drebrin A.

Our pyrene florescence assays suggested that drebrin’s C-terminal part may bind to mDia2 FH1-FH2 region (Fig.7a and 7b). We also demonstrated that drebrin A inhibits actin nucleation by mDia2 formin (Fig.3a). Because formin’s FH2 domain is critical for actin nucleation, whereas the FH1 domain recruits profilin bound G-actin, we hypothesized that drebrin’s C-terminal region most likely interacts with the FH2 domain to disrupt mDia2-driven actin nucleation. Ideally, we would perform this experiment with the purified C-terminal part of drebrin (residues 301-706) and mDia2-FH2 domain. However, the C-terminal part of drebrin is intrinsically disordered making it very difficult to express and purify from E. coli cells. To overcome this technical difficulty, we decided to compare DrbFL and Drb1-300 in pull-down assays. If our hypothesis is correct, only DrbFL but not Drb1-300 would interact with mDia2-FH2 domain. In order to test this directly we performed a pull-down where immobilized GST fused full-length drebrin was incubated with mDia2-FH2 (Fig.10). Our pull-down revealed direct binding with a molar binding ratio of 1:1 (N=3) between full-length drebrin and mDia2-FH2. Next, we wanted to confirm that Drb1-300 construct does not interact with the FH2 domain of mDia2. We incubated immobilized GST fused Drb1-300 with mDia2-FH2 (Fig.10). We pulled down slightly more mDia2-FH2 on GST-Drb1-300 as compared to GST alone but significantly less than with full-length drebrin. It is possible that Drb1-300 may weakly bind mDia2-FH2 in a nonspecific manner. Additional experiments will be needed to confirm or rule out this possibility. Thus, our pull-down experiments suggest that the FH2 domain of mDia2 directly binds to the C-terminal region of drebrin A.

Drebrin A inhibits mDia2-mediated F-actin bundling. Formins not only nucleate and elongate actin, but some also display F-actin side binding. mDia2 is a formin that is capable of

side binding and bundling F-actin [33]. In order determine if drebrin A affects actin bundling by the mDia2-FH2 domain we performed a series of low-speed pelleting assays, in which bundled F-actin pellets while single filaments remain in the supernatant. As previously shown [33], mDia2-FH2 causes actin bundling in a concentration dependent manner (Fig.11). Interestingly, full-length drebrin A inhibits mDia2-FH2 bundling activity, with less actin detected in the pellet (Fig.12a). Drebrin's inhibition of mDia2-FH2 bundling activity is concentration dependent (Fig.13). To determine the domain requirement for drebrin's inhibition of mDia2 bundling activity, we performed low speed pelleting experiments with truncated drebrin constructs. Unlike full-length drebrin, drebrin's N-terminal constructs (Drb1-300, Drb2-252) do not affect actin bundling by mDia2-FH2 (Fig.12b and 12c). This supports our hypothesis that drebrin's C-terminal part binds the mDia2-FH2 domain.

To better understand the mechanism of unbundling by drebrin we tested the effects of a phosphomimetic drebrin A mutant (DrbS142D, Fig.1d) on actin bundling by formin. Based on *in vivo* work, it was proposed that mutating residue 142 from serine to aspartate causes changes in drebrin's conformation such that it is more "open" as opposed to "closed" [34]. Our data indicates that mimicking phosphorylation at drebrin's serine-142 residue does not alter its inhibitory effect on mDia2-FH2 bundling activity (Fig.14). Thus, drebrin's inhibition of actin bundling by mDia2-FH2 is not regulated by drebrin's phosphorylation on S142.

Drebrin A and mDia2 formin co-decorate actin filaments. We hypothesized that drebrin inhibits mDia2 actin bundling activity by displacing mDia2-FH2 from actin filaments. To investigate this possibility we performed a high-speed pelleting assay, in which all proteins bound to actin filaments pellet, while those that did not bind actin filaments remain in the supernatant. Our assay was consistent with previous reports, showing that mDia2-FH2 binds F-actin and is visible in high-speed pellets. All drebrin constructs tested (DrbFL, Drb1-300, Drb2-252) bind F-actin and co-pellet with it. When drebrin constructs were introduced in the presence of mDia2-FH2 both were visible in the pellet, indicating that the drebrin constructs and mDia2-

FH2 co-bind to F-actin (Fig.15a). However, full-length drebrin (1uM) displaces mDia2-FH2 from actin filaments, leaving on average 0.45uM FH2 bound to F-actin (Fig.15b). Drebrin's N-terminal constructs (Drb1-300, Drb2-252) do not displace mDia2-FH2 to this extent. Based on our low speed pelleting mDia2-FH2 concentration dependence, 0.45uM mDia2-FH2 would be sufficient to bundle actin (~70% bundled, Fig.11b). However, when full-length drebrin was added to mDia2-FH2-bound F-actin, bundling activity was nearly abolished (~10% bundled at 1uMDrbFL, Fig.13b). Thus, our data suggests that drebrin A prevents mDia2-FH2-mediated bundling of actin not by competing it off the filaments, but by directly interacting with the FH2 domain and preventing it from binding to two filaments simultaneously.

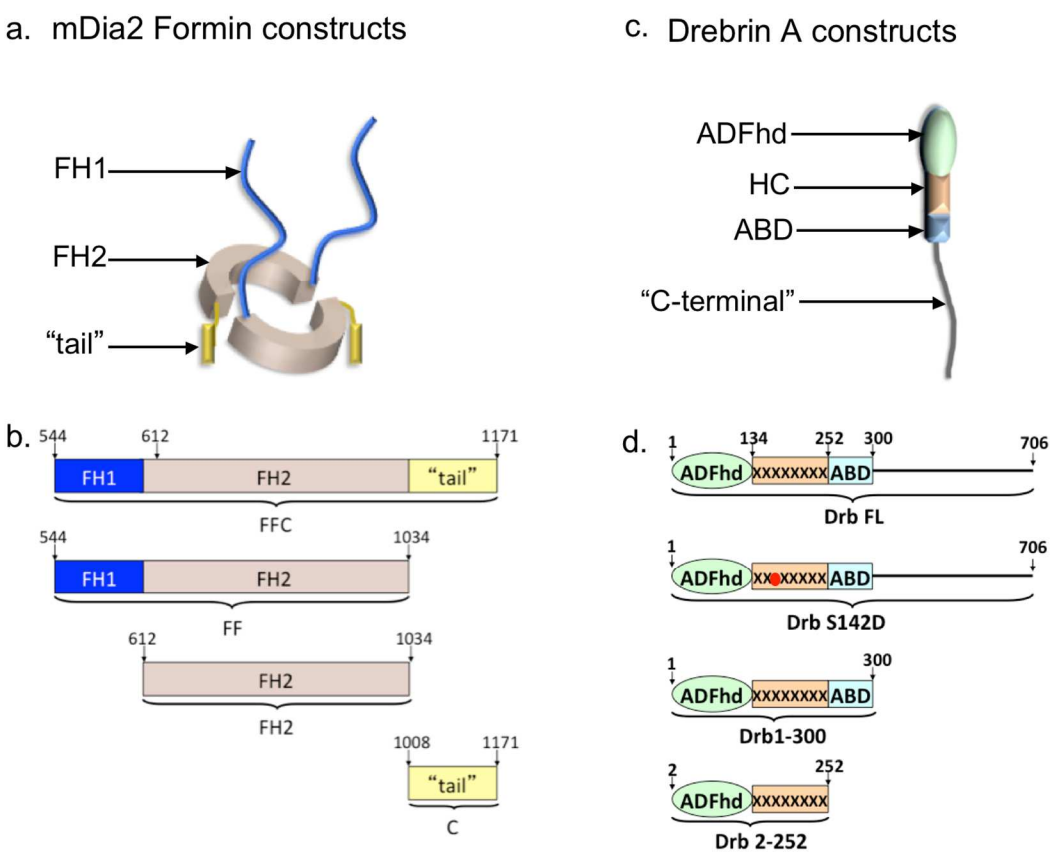

FIGURE 2: **Schematic representation of drebrin A and mDia2 formin constructs used in this study.**

(a) Schematic 3D representation of the C-terminal part of mDia2 containing FH1, FH2 and "tail" region (FFC). Formin exists in the form of an antiparallel dimer formed by two FH2 domains. mDia2 can promote actin nucleation and also bind to filaments' barbed ends and sides. FH1 domains contain poly proline-rich regions that bind profilin-actin to increase local actin concentration near the barbed ends of filaments. FH1 domain is required for processive formin-driven actin elongation from profilin-actin complexes. The FFC construct is most efficient in promoting actin nucleation because it contains the FH2 domain (sufficient for actin nucleation) and C-terminal "tail" (aids nucleation and processive actin elongation).

(b) Schematic representation of mDia2 formin constructs used in this study: FH1 domain (blue box), FH2 domain (beige box), C-terminal "tail" (which contains the diaphanous auto-regulatory domain; DAD) (yellow box).

(c-d) Diagram of drebrin A constructs, showing the ADFhd domain (actin depolymerizing factor homology domain, green oval), helical-charged domain (HC, orange box), ABD domain (actin-binding domain, blue box), and the disordered C-terminal region (black line). Red dot corresponds to the location of phosphomimetic mutation S142D.

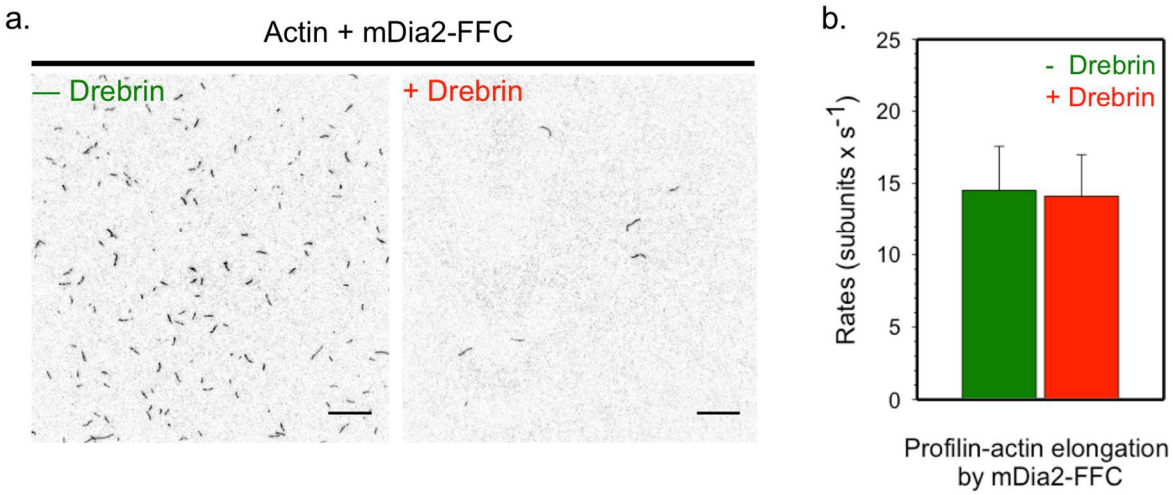

FIGURE 3: **Drebrin A inhibits mDia2 formin-dependent actin nucleation, but not processive elongation with profilin-actin.**

(a) TIRFM images of actin filaments nucleated by mDia2-FFC in the absence (left) and in the presence of drebrin (right). We detected a dramatic decrease in number of actin filaments in the presence of drebrin than with mDia2-FFC alone. Scale bar: 10um.

Conditions: [Actin]=1uM (15% Alexa488-SE labeled), [mDia2-FFC]=30nM, [drebrin]=1.2uM. Buffer: 10mM HEPES pH7, 1mM EGTA, 1mM $MgCl_2$, and 50mM KCl, 0.2mM ATP, 1mM DTT (**KMEH7**).

(b) Quantification of the single filament actin elongation assays with and without drebrin A. Untethered actin filaments were imaged on Pluronic coated slide surface. Imaging buffer was supplemented with 0.5% methylcellulose to hold filaments close to the slide surface. The rate of profilin-actin elongation does not change when drebrin is added (red bar: 14.1+/-2.9 subunits/s, n=24 filaments; green bar: 14.5+/-3.1 subunits/s, n=21 filament). Error bars: standard deviation. Thus, drebrin does not affect actin elongation from profilin-actin by mDia2 formin.

Conditions for time lapse TIRF experiments: [Actin]=0.5uM (15% Alexa488-SE labeled), [profilin]=2.5uM, [mDia2-FFC]=1.5nM, [drebrin A]=0.73uM. Buffer: KMEH7.

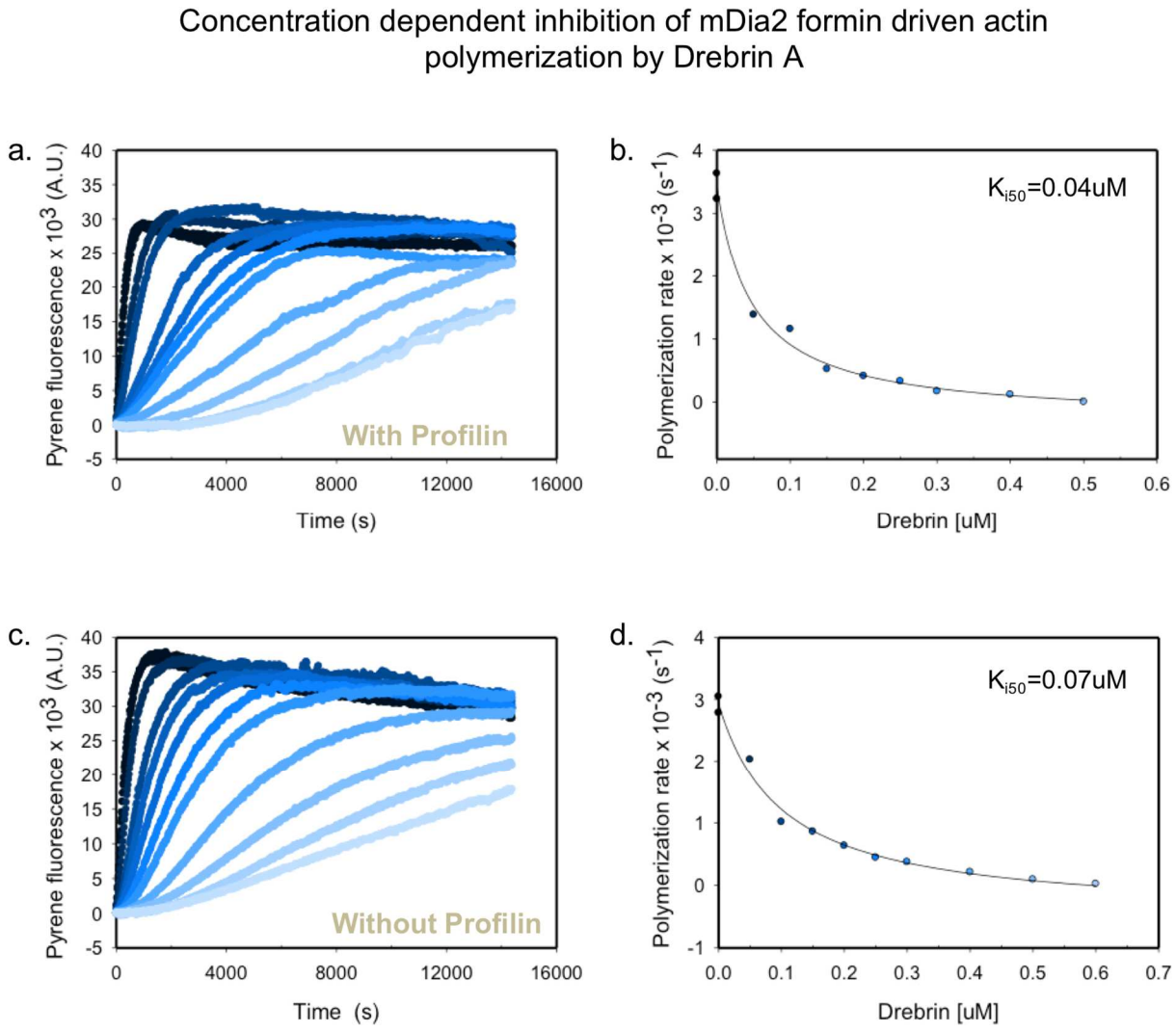

FIGURE 4: **Full length drebrin A concentration dependent inhibition of actin polymerization driven by the mDia2-FFC construct.**

(a) Drebrin A inhibits mDia2-FFC-driven polymerization of actin in the presence of profilin. mDia2 formin accelerates profilin-actin polymerization in the absence of DrbFL (black trace) as indicated by the increase of pyrene fluorescence signal. The shift from dark blue to light blue represents increasing drebrin concentrations (0.05, 0.10, 0.15, 0.2, 0.25, 0.3, 0.4, 0.5, 0.6, and 0.7uM). As the concentration of drebrin increases, the rate of actin polymerization decreases.

(b) Quantification of the data shown in (a). Plotting actin polymerization rates against DrbFL concentration indicates the drebrin concentration necessary to achieve half maximum inhibition of actin polymerization is 0.04uM.

(c-d) Drebrin A inhibits mDia2-FFC-driven polymerization of actin in the absence of profilin. The same effect is observed without profilin, with 0.07uM DrbFL necessary to achieve half maximum inhibition of the rate of polymerization.

Conditions: [Actin]=1uM (10% pyrene-maleimide), [profilin]=5uM, [mDia2-FFC]=30nM. Buffer: KMEH7.

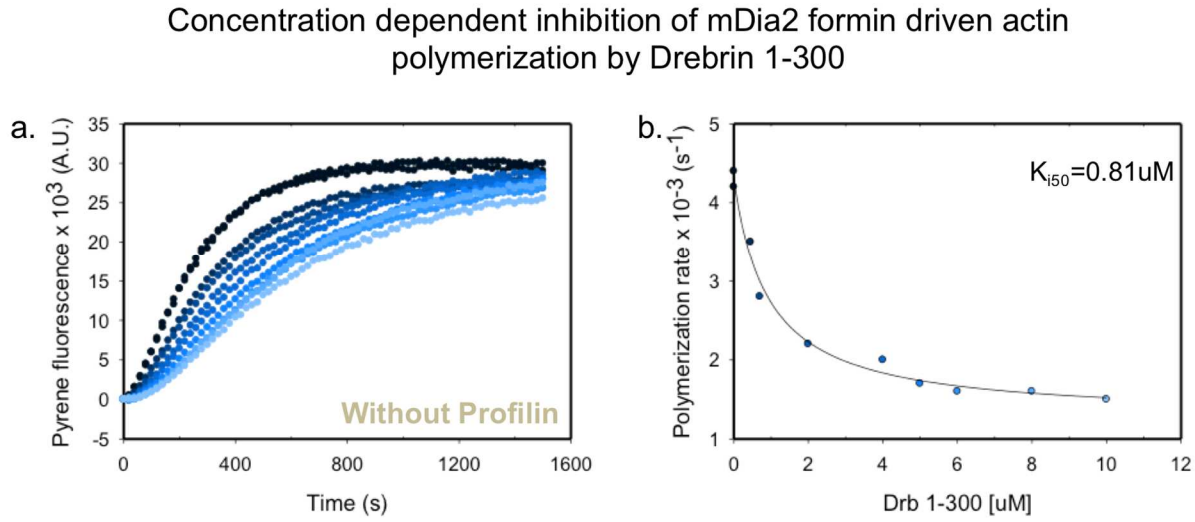

FIGURE 5: **Drebrin 1-300 concentration dependent inhibition of mDia2-FFC driven actin polymerization.**

(a) Drb1-300 inhibits mDia2-FFC-driven polymerization of actin. The shift from dark blue to light blue corresponds to increasing concentrations of Drb1-300 (0, 0.45, 0.7, 2, 4, 5, 6, 8, and 10uM).

(b) Quantification of the data shown in (a). Plotting polymerization rates against Drb1-300 concentration indicates that 0.81uM Drb1-300 is necessary to attain half maximum inhibition of actin polymerization.

Conditions: [Actin]=1uM (10% pyrene-maleimide), [mDia2-FFC]=30nM. Buffer: KMEH7.

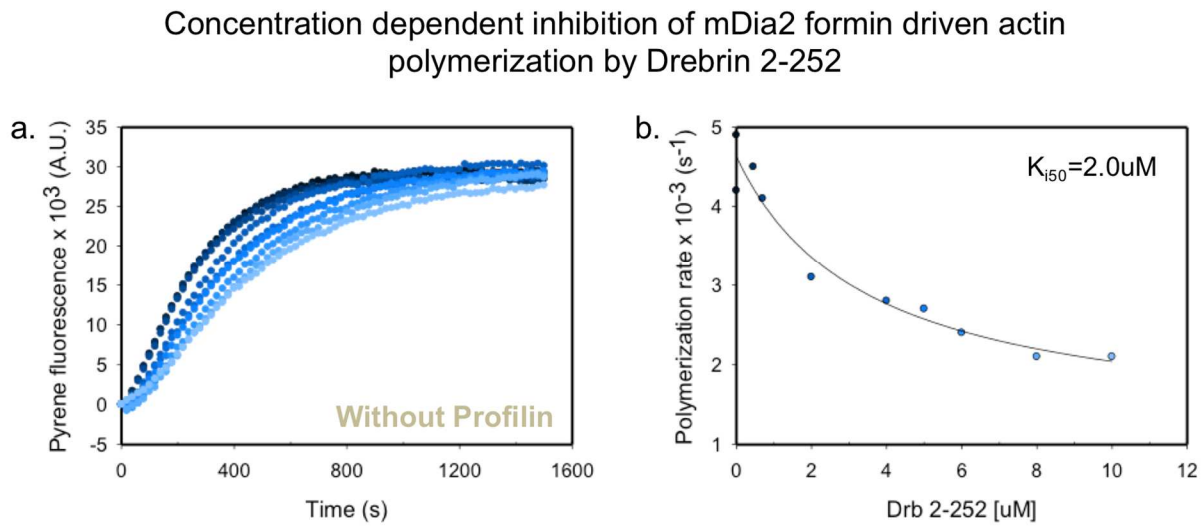

FIGURE 6: **Drebrin 2-252 concentration dependent inhibition of mDia2-FFC driven actin polymerization.**

(a) Drb2-252 inhibits mDia2-FFC-driven polymerization of actin. The shift from dark blue to light blue represents increasing concentration of Drb2-252 (0, 0.45, 0.7, 2, 4, 5, 6, 8, and 10uM).

(b) Quantification of the data shown in (a). Plotting polymerization rates against Drb2-252 concentration indicates that 2.0uM Drb2-252 is necessary to attain half maximum inhibition of actin polymerization.

Conditions: [Actin]=1uM (10% pyrene-maleimide), [mDia2-FFC]=30nM. Buffer: KMEH7.

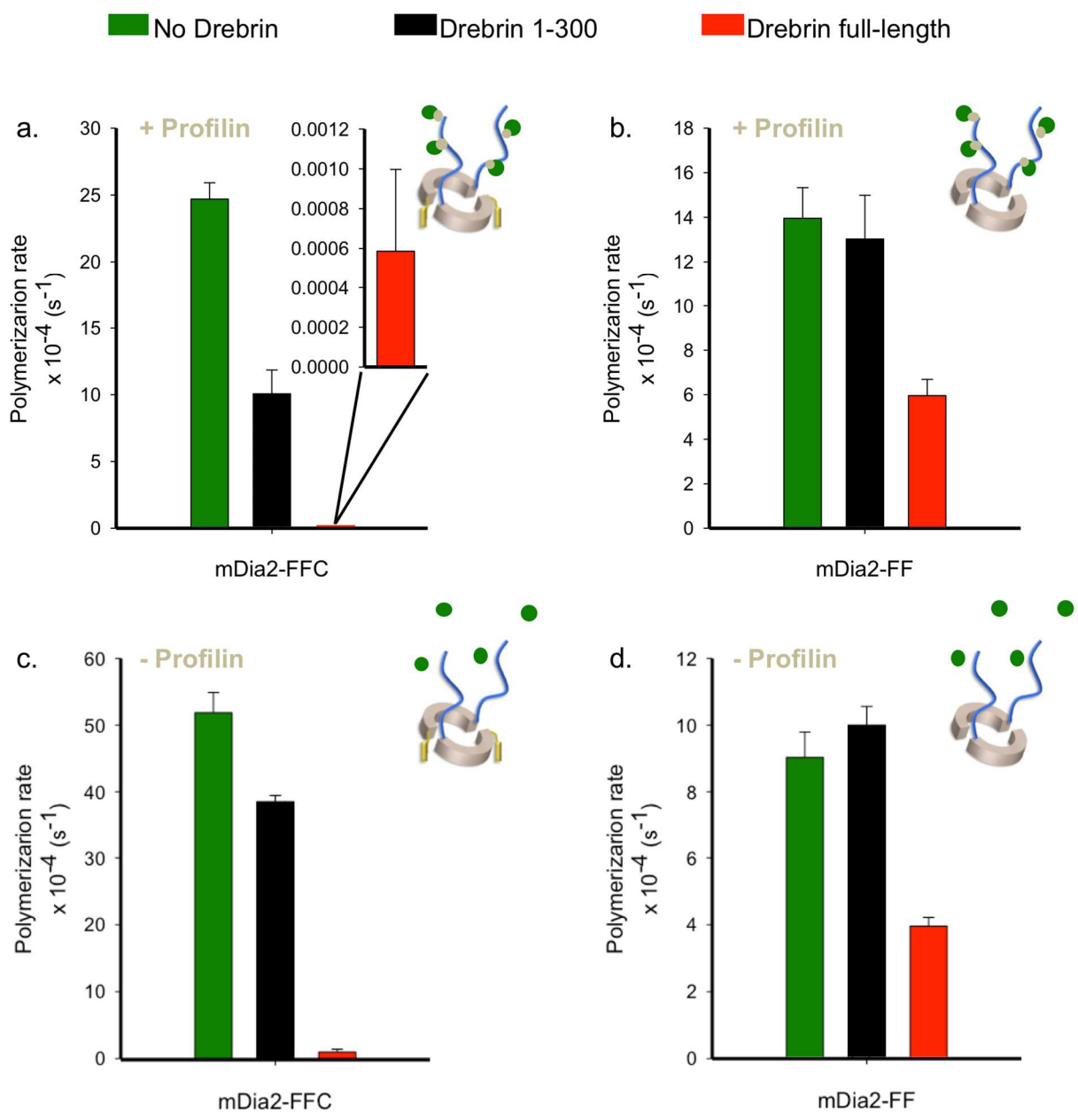

FIGURE 7: **Identifying mDia2 region(s) affected by drebrin A.**

(Continued on the following page.)

FIGURE 7: **Identifying mDia2 region(s) affected by drebrin A.** (Continued)

The effect of full length drebrin and Drb1-300 ("actin-binding core") on the rates of actin polymerization driven by mDia2-FFC and mDia2-FF constructs was tested here. mDia-FF is lacking the C-terminal "tail" region, which is shown to aid formin-driven actin nucleation and processive elongation. Schematic representations of formin constructs used are placed next to each panel. In these schematics actin and profilin are represented by green and beige spheres, respectively. Actin polymerization rates were determined in pyrene fluorescence assays.

(a) Polymerization of profilin-actin complex driven by mDia2-FFC constructs is inhibited in the presence of full length drebrin. This inhibition is reduced but not abolished in the presence of its "actin-binding core" Drb1-300.

(b) Profilin-actin polymerization driven by mDia2-FF constructs is inhibited by full length drebrin but not by Drb1-300

(c-d) Experiments in (a) and (b) were repeated without profilin and yielded similar results. Representative sets of data are shown. Error bars=standard deviation (N=3 samples).

Conditions: [Actin]=1uM (10% pyrene-maleimide), [profilin]=5uM, [mDia2-FFC/FF]=30nM, [Drebrin FL]=0.7uM, [Drb1-300]=1.6uM. Buffer: KMEH7.

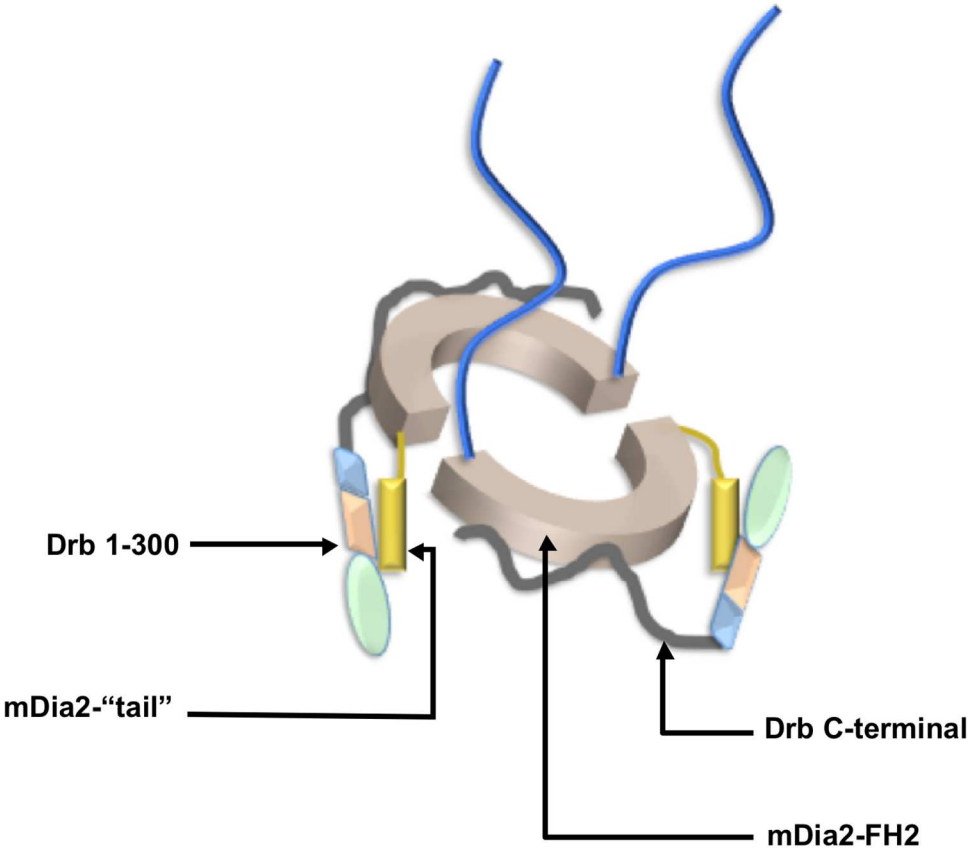

FIGURE 8: **Hypothetical model of mDia2-FFC formin and full length drebrin A interaction.**

We propose this model based on the results of our pyrene florescence assays. Based on these assays “tails” of mDia2 may interact with “actin binding core” of drebrin (Drb1-300), while the FH2 domain of mDia2 may interact with the intrinsically disordered C-terminal region of drebrin. We set out to test this model in direct pull-down experiments (see Fig.9 and 10).

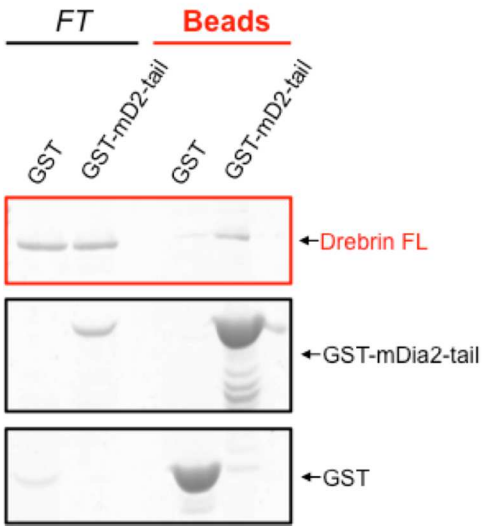

FIGURE 9: **Full length drebrin A binds mDia2-C terminal "tails".**

Pull-down samples were prepared by adding 1uM full length drebrin to either GST (2uM), or GST-mDia2-"tails" (2uM). Samples were incubated with Glutathione sepharose beads for 2 hours at 4ºC. Flow through (*FT*, first two lanes) and beads (lanes 3-4) were analyzed by SDS PAGE.

Buffer: KMEH7 supplemented with 0.5mM thesit. Gel was stained with Coomassie blue.

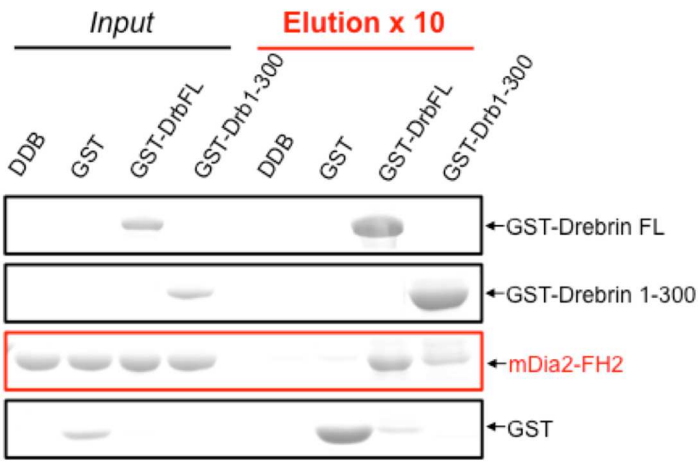

FIGURE 10: **Full length drebrin A directly binds mDia2-FH2.**

For pull down experiments 1uM of GST, GST-drebrin full length, or GST-Drb1-300 were incubated with 2uM mDia2-FH2 at 4^{o}C overnight (lanes 1-4, *Input*). Then, these samples were applied onto Glutathione sepharose beads and incubated for 3 hours at 4^{o}C. After a wash with the assay buffer, proteins were eluted from the beads with 1/10th of the original volume of glutathione (lanes 5-8, *Elution x 10*) and analyzed by SDS PAGE. Arrows and labels on the right side identify the resulting gel bands. Note, that mDia2-FH2 does not bind to the beads or GST alone (lanes 5-6, 3d panel from the top), but co-elutes with GST-drebrin full length (lane 7, 3d panel from the top) and (in much lesser amount) with GST-Drb1-300.

Buffer: KMEH7, 0.5mM thesit, 0.05% Igepal-CA-630; details of the assay are provided in *Materials and Methods* section. Gel was stained with Coomassie blue.

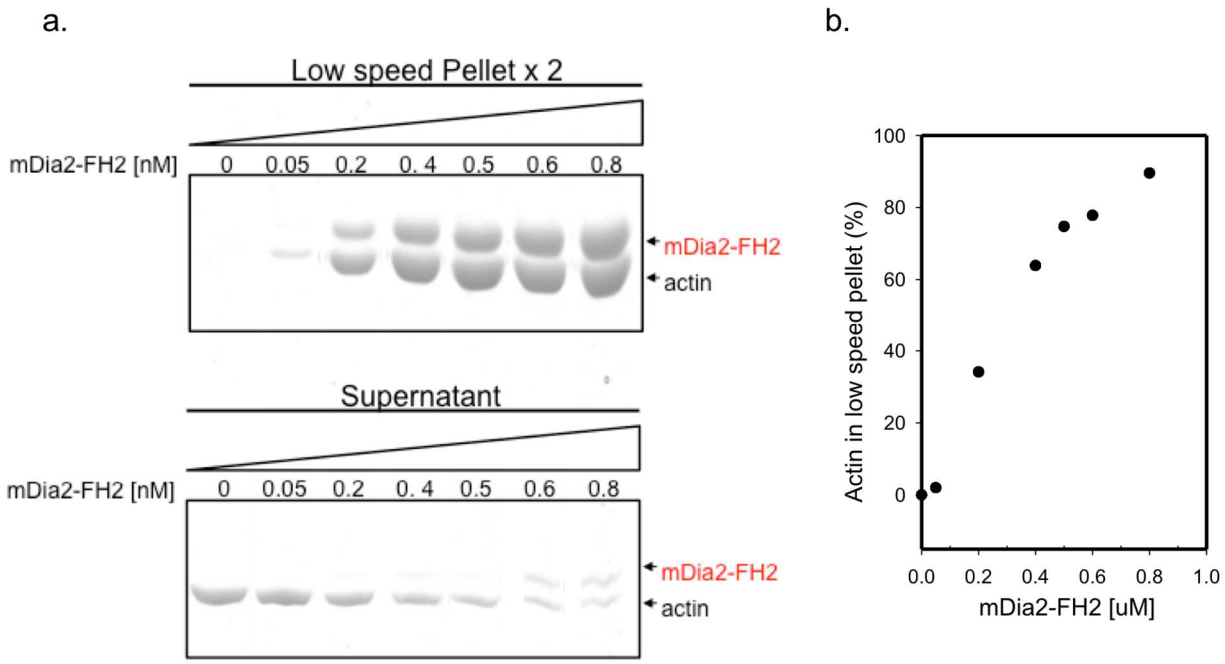

FIGURE 11: **mDia2-FH2 bundles actin filaments.**

(a) Low speed pelleting and SDS PAGE analysis of filamentous actin (2uM, polymerized overnight at 4^{o}C) in the presence of increasing concentrations of mDia2-FH2 (0, 0.05, 0.2, 0.4, 0.5, 0.6, and 0.8uM). Samples were incubated at room temperature for 1 hour before centrifugation (16,000xg, 5min, 4^{o}C). As mDia2-FH2 concentration increases the amount of actin bundled (detected in the low speed pellet) increases. Top and bottom panels show SDS PAGE analysis of low speed pellets and supernatants, respectively.

(b) Quantification of the data shown in (a, top panel).

Buffer: KMEH7. Gel was stained with Coomassie blue. Note, that pellets were concentrated two fold to aid quantification.

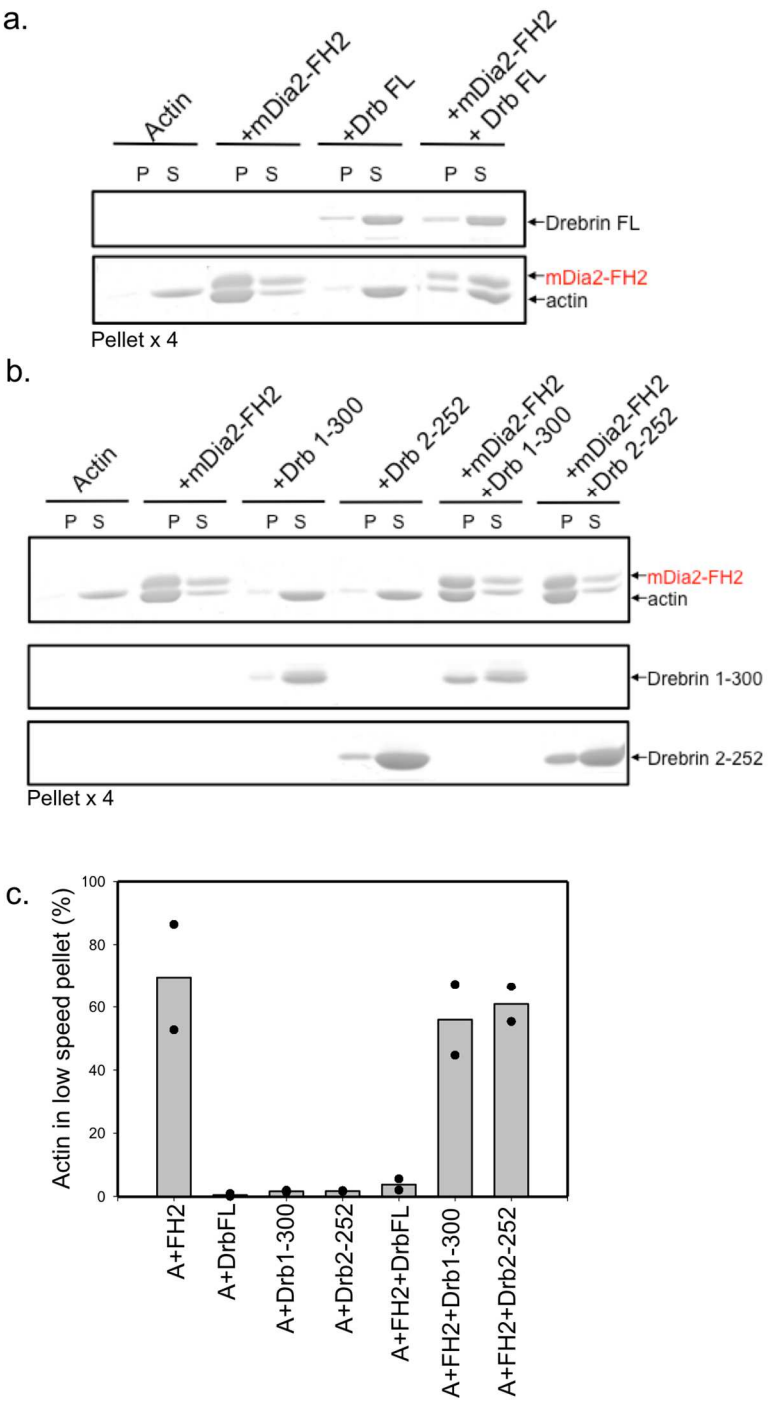

FIGURE12: **Full length drebrin A strongly inhibits mDia2-FH2-mediated bundling of F-actin.**

(Continued on the following page.)

FIGURE12: **Full length drebrin A strongly inhibits mDia2-FH2-mediated bundling of F-actin.** (Continued)
(a-b) Low speed pelleting and SDS PAGE analysis of F-actin in the presence of mDia2-FH2 (0.8uM) and different drebrin constructs.
(a) Low speed pelleting and SDS PAGE analysis of F-actin in the presence of mDia2-FH2 and 1uM full length drebrin. Representative gel is shown. Judging from low speed pelleting assays, no bundling (actin in pellets) was detected with actin alone (lanes 1-2) and with F-actin-DrbFL complex (lanes 5-6). In contrast, most of the actin was found in low speed pellets in the presence of FH2 (lanes 3-4, also see Fig.11). However, full-length drebrin strongly inhibited mDia2-FH2 mediated bundling - no actin was detected in the low speed pellets (lanes 7-8).
(b) Low speed pelleting and SDS PAGE analysis of F-actin in the presence of mDia2-FH2 and N-terminal drebrin constructs – Drb1-300 and Drb2-252. Representative gel is shown. Under our experimental conditions, the extent of actin bundling (actin in pellets) was negligible with Drb1-300 and Drb2-252 in the absence of mDia2-FH2 (lanes 5-6 and 7-8, respectively). Gel analysis showed that Drb1-300 and Drb2-252 did not affect the extent of F-actin bundling by mDia2-FH2 (lanes 9-12), as opposed to full length drebrin (panel (a), lanes 7-8).
(c) Quantification of data shown in (a) and (b). Bar graphs are the averages of 2 independent experiments (per condition). Individual values obtained in each repeat are shown in the same graph (black dots).

Conditions: [F-actin-phalloidin]=2uM, actin, (1:1 complex with phalloidin). Pellets were concentrated four fold to aid quantification. Buffer: KMEH7**.** Gel was stained with Coomassie blue.

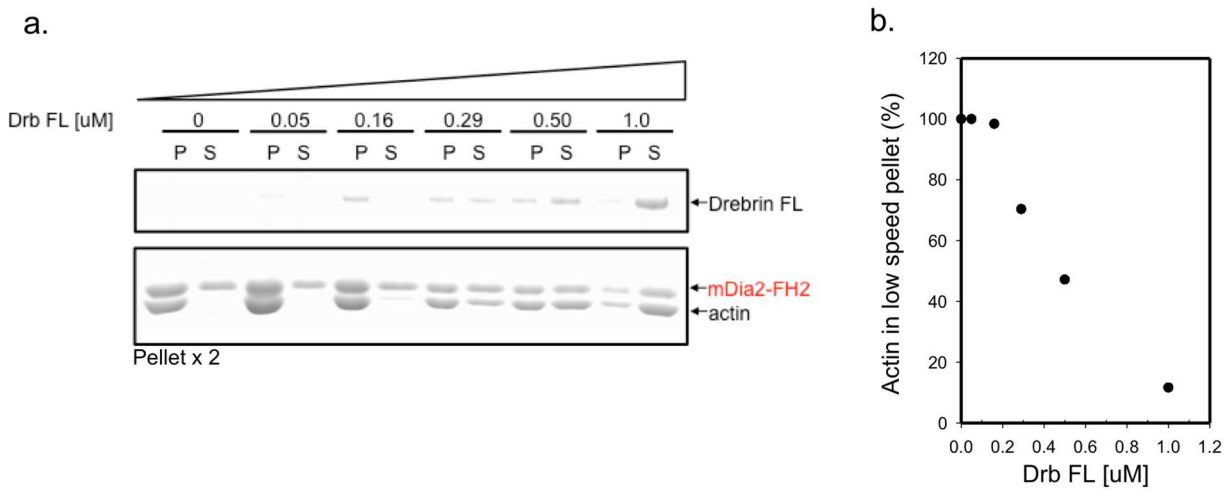

FIGURE 13: **Inhibitory effect of drebrin A on mDia2-FH2-mediated bundling is concentration-dependent.**

(a) Low speed pelleting and SDS PAGE analysis of F-actin in the presence of mDia2-FH2 and increasing concentrations of full length drebrin. Representative gel is shown. Pellets were concentrated two fold to aid quantification.

(b) Quantification of data shown in (a).

Buffer: KMEH7. Gels were stained with Coomassie blue.

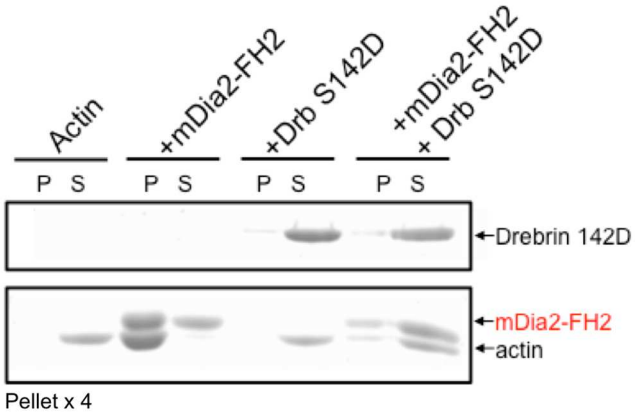

FIGURE 14: **Phosphomimetic mutant of drebrin A (S142D) also strongly inhibits mDia2-FH2-mediated bundling of F-actin.** Low speed pelleting and SDS PAGE analysis of F-actin in the presence of mDia2-FH2 (0.8uM) and 1uM drebrin S142D (DrbS142D). A representative gel is shown. DrbS142D did not bundle actin in the absence or in the presence of mDia2-FH2. Thus, like full-length drebrin, the S142D mutant also inhibits mDia2-FH2 mediated actin bundling.

Buffer: KMEH7. Gels were stained with Coomassie blue. Pellets were concentrated four fold to aid quantification.

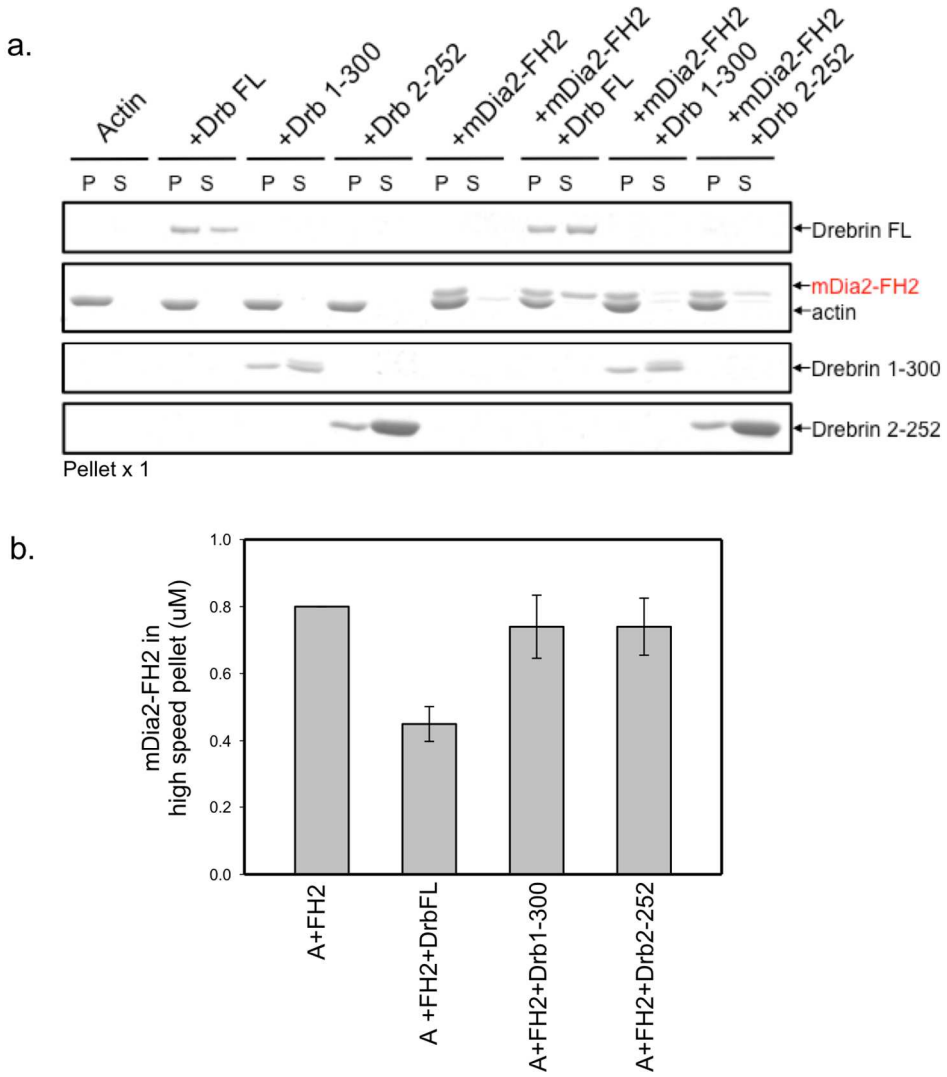

FIGURE 15: **Drebrin A constructs and mDia2-FH2 co-bind filamentous actin.**

(a) High speed pelleting of F-actin in the presence of mDia2-FH2, and drebrin constructs (full length drebrin, Drb1-300, or Drb2-252). F-actin alone was found in high speed pellet (lanes 1-2). All drebrin constructs used bind F-actin (present in the high speed pellets; lanes 3-8). mDia2-FH2 binds F-actin (present in high speed pellet; lanes 9-10). All drebrin constructs employed co-bind actin with mDia2-FH2 (both, drebrin constructs and mDia2-FH2 were detected in high speed pellets; lanes 11-16). Full length drebrin, unlike the N-terminal constructs, partially displaces mDia2-FH2 such that some FH2 can be detected in supernatants (lane 12).

(b) Quantification of data shown in (a).

Conditions: [F-actin]=2uM; [mDia-FH2]=0.8uM, [drebrin constructs]=1uM. Buffer: KMEH7. Gels were stained with Coomassie blue.

Discussion

In this work we identified neuron-specific drebrin A as a new interacting partner for mDia2 formin. Both drebrin's N-terminal ("actin binding core") and C-terminal (intrinsically disordered) regions appear to be involved in its interaction with mDia2. Our results suggest the existence of two drebrin binding sites on mDia2 formin – one in the FH2 domain and another in the "tail" region (Fig.8). Upon their direct interaction, drebrin inhibits mDia2-driven actin nucleation, which is mediated via the FH2 domain and aided by the "tail" region of formin. However, processive actin-elongation by mDia2 is not affected in the presence of drebrin. Moreover, F-actin bundling activity of mDia2 (known to be mediated via its FH2 domain) is abolished by drebrin.

The mechanism of actin bundling mediated by formin's FH2 domain has not been elucidated yet [19, 33]. However, it is likely that the FH2 homodimer bundles actin by interacting with actin filaments through two actin binding sites (one in each FH2 domain) [33]. We hypothesize that drebrin may abolish formin bundling activity through its C-terminal segment interaction with mDia2 formin's FH2 domain (as confirmed by our pull-down assays, Fig.10). Drebrin's C-terminal segment may mask one or both actin interacting sites on mDia2-FH2, thus interfering with formin's bundling activity. If drebrin's C-terminal masks both actin interacting sites on mDia2-FH2, then it can interfere with the FH2 domain binding to actin filaments. This scenario is consistent with our high speed pelleting data in which full length drebrin, unlike its N-terminal constructs, partially displaces mDa2-FH2 off F-actin (Fig.15).

The expression level of mDia formins rises during neuritogenesis and dendritic spine formation [20]. Specifically, mDia2 expression increases during the development of dendritic filopodia, a precursor of dendritic spines [20]. During spine maturation, actin architecture in heads of the spines changes from mostly linear arrays to Arp2/3 branched networks that form the drebrin-rich "core" of the spine [35]. It is possible that drebrin enrichment in dendritic spines is needed to suppress formin driven actin nucleation and restrict the activity of formins to actin

elongation, thereby favoring Arp2/3 branching in mature spines. In line with this, constitutively active mDia2 formin induces the loss of dendritic spine heads *in vivo* [20]. Thus, the mDia2-drebrin A interaction may be important for the development and maintenance of actin architecture in the stable "core" of dendritic spines.

In the future it will be important to map the drebrin-mDia2 interacting interface(s). The benefits of identifying the residue(s) necessary for drebrin-mDia2 interaction are two-fold. (1) Mapping drebrin-mDia2 binding site(s) can help us better understand how their direct binding may affect their cross-talk with other regulators involved in dendritic spine maturation. (2) Once we have identified the residues required for this interaction, we can target them for substitutions, which would disturb drebrin-mDia2 binding *in vivo* while preserving their other interactions, and observe changes in the spine phenotype.

It is known that the transition from embryonic drebrin to its adult isoform is necessary for the maturation of filopodia into spines [6, 11]. Differences in their interaction with mDia2 (and possibly other formins) may be important during brain development. Drebrin A contains a neuron-specific sequence (ins2) in its C-terminal region, which is missing in Drebrin E [11]. We identified the C-terminal of drebrin as a likely interface for mDia2 binding. We cannot exclude that this formin interaction site of drebrin is located in neuron-specific sequence (ins2) of the molecule. Thus, potentially, drebrin isoforms can interact with mDia2 differently, which may be important for spine development.

In another aspect of mDia2 function, its "tails" were shown to be important for binding to microtubules [19, 27]. Because our data suggest that drebrin may interact with the mDia2-"tails" (Fig.8), it would be interesting to explore the possibility that drebrin-mDia2 interaction interferes with microtubule binding of mDia2.

Materials and Methods

Proteins

Rabbit skeletal actin (RSA) [36], profilin [37], full length drebrin [31], Drb1-300 construct [30], Drb2-252 [17], were expressed and purified as described previously. The mDia2-FFC plasmid was a generous gift from Dr. H. Higgs [33]. mDia2-FF construct was created via mutagenesis, with primers designed to introduce a stop codon after the FH2 domain (residue 1034). mDia2 FFC, FF, and "tail" constructs were expressed as N-terminal GST fusion proteins in E. coli (Rosetta2 competent cells) [38]. Purification of the formin constructs was carried out essentially as described [38] except the last step when gel-filtration was performed instead of ion exchange chromatography. In brief, formin constructs were purified on Glutathione sepharose column, and cleaved with thrombin, overnight, at 4°C. Cleaved formin constructs were further purified using gel filtration on HiLoad 16/60 Superdex 75 (Amersham Biosciences). The mDia2-FH2 construct was a kind gift from Dr. M. Quinlan's lab (Dr. Christina Vizcarra).

TIRF Microscopy

TIRF imaging of F-actin immobilized on polylysine-coated surface. Coverslips were treated with 1mg/ml polyK for 3 min, rinsed with mQ water and air-dried. Mg-ATP-G-actin (0.9 uM 15% Alexa488-SE labeled [39]) was polymerized in **KMEH7** (50mM KCl, 1mM $MgCl_2$, 1mM EGTA, 10uM HEPES, pH7; 1mM DTT, 0.2mM ATP) in the presence of mDia2-FFC (30nM) ± drebrin A (1.2uM). After 10 min at room temperature, samples were diluted 67-fold in KMEH7, supplemented with 100 mM DTT and 1uM phalloidin, and applied onto polylysine surface. Random fields were imaged using DMI6000 TIRF microscope (Leica).

Time lapse TIRF microscopy. Untethered actin filaments were imaged on Pluronic coated surface as described [39, 40]. Flow chambers (V~12µl) were assembled using a single layer of permanent double-sided Scotch tape. For each sample the flow chamber was treated with 2 chamber volumes (CV) of 1% Pluronic F127 solution (Sigma, P2443) for 3 min, then

equilibrated with 2 CV of 1xTIRF imaging buffer (10mM HEPES, 1mM $MgCl_2$, 50mM KCl, 0.2mM EGTA (pH 7) supplemented with 50mM DTT, 0.2mM ATP, 20mM glucose, 0.5% methyl cellulose). G-actin-profilin mixtures (1uM 15% Alexa488-SE labeled actin, 5uM human profilin-1) were incubated for 3 min at RT with Mg/EGTA exchange buffer (0.2mM EGTA, 50μM $MgCl_2$). Then, Mg-ATP-G-actin in complex with profilin was mixed with polymerizing salts supplemented with mDia2-FFC (2nM), with and without DrbFL (0.7uM). The resulting mixture (4 CV) was introduced into the flow chamber. Actin mixtures were supplemented with 0.05mg/ml caseine, 0.25mg/ml glucose oxidase, 50μM catalase to minimize damage due to radicalization and photobleaching during imaging. Filaments were imaged using DMI6000 TIRF microscope (Leica). Images were acquired every 5-10 sec. All TIRF data were analyzed using ImageJ (Fiji) software (NIH, Bethesda, MD).

Actin polymerization assays

Mg-ATP G-actin (10% pyrene-maleimide) was prepared by incubating Ca-ATP-G-actin with ME buffer (0.05 mM $MgCl_2$ and 0.2 mM EGTA) for 3 minutes. Actin polymerization was initiated immediately after Ca/Mg exchange by simultaneous addition of polymerization buffer KMEH7 and actin-binding proteins (profilin, drebrin and formin constructs). Average delay between beginning of actin polymerizations and first measurement was ~35s. Changes in pyrene fluorescence signal were monitored over time (1-4 hours) using a microplate reading fluorimeter (TECAN). SigmaPlot software was used to fit actin polymerization kinetics to exponential expressions yielding polymerization rates and their standard deviations.

Pull-down assays

Pull-down experiments with GST-mDia2-tails. For pull-down experiments GST-fused mDia2-tail and GST were incubated with DrbFL (~10min, 25^{o}C) in **T-KMEH7** buffer (KMEH7, 1mM DTT, 0.5mM thesit). Samples were applied onto Glutathione sepharose beads (equilibrated with T-

KMEH7) and nutated at 4°C for 2 h. Beads were precipitated by centrifugation (14,000 rpm, 2 min, 4°C) and supernatant (flow trough) collected for analysis (see Fig.9, *FT*). Beads were washed 3 times with 8 column volumes of T-KMEH7 (24 column volumes total). After washes beads were pelleted by centrifugation and re-suspended in 1 column volume of T-KMEH7. Supernatants and bead suspensions were supplemented with SDS PAGE sample loading buffer, boiled for 3 min, and resulting samples were analyzed by SDS PAGE. Gels were stained with Coomassie blue.

Pull-down experiments with GST-drebrin constructs. GST-fused FL drebrin, GST-fused Drb 1-300, GST, or drebrin dialysis buffer alone (**DDB**: 5mM TRIS pH8, 100mM KCl, 1mM DTT) were each incubated overnight at 4°C with mDia2-FH2 in **IT-KMEH7** (KMEH7, 1mM DTT, 0.05% IGEPAL CA 630, 0.5mM thesit). Resulting samples (*Inputs*, Fig.10) were applied onto glutathione-sepharose beads (equilibrated with IT-KMEH7) and nutated at 4°C for 3h. Beads were pelleted using a bench-top centrifuge, then washed one time with 5 column volumes of IT-KMEH7. Beads were incubated with 10mM glutathione elution buffer (~2 column volumes) for 5min at 25°C. Inputs and eluates were analyzed by SDS PAGE (10%gels) and stained with Coomassie blue.

High and Low speed pelleting assays

High speed pelleting assay. Mg-ATP F-actin (5uM) was prepared by incubating Ca-ATP-G-actin with the **ME** buffer (0.05 mM $MgCl_2$ and 0.2 mM EGTA) for 3 minutes, followed by incubation in a polymerizing buffer (KMEH7, 1.8mM Tris, 1mM DTT, 0.2mM ATP) at 4°C overnight. This actin stock was then diluted to 2uM with a polymerization buffer (KMEH7, 1mM DTT, 0.2mM ATP) in the presence or absence of mDia2-FH2 (0.8uM) and drebrin constructs (at concentrations that correspond to ≥80% occupancy: [Drb FL]= 0.85-1uM, [Drb 1-300]=1.9uM, [Drb 2-252]= 12.7-19.8uM). Reaction mixtures were incubated at RT for 10 min and then subjected to high speed centrifugation (TLA100, 80,000 rpm, 4°C, 20 min). Supernatants and pellets were analyzed by

SDS PAGE. Gels were stained with Coomassie Blue. Scion Image software was used to determine the intensities of the gel bands.

Low speed pelleting assay. Low speed pelleting assays were carried out as described for high speed pelleting with the following modifications. Mg-ATP F-actin (5uM) was supplemented with Phalloidin (5uM). Reaction mixtures were incubated at RT for 1h then subjected to low speed centrifugation (16,000 x g, 4^{o}C, 5 min).

Partial denaturation of full-length drebrin

We encountered technical difficulties with several FL drebrin preparations; specifically, drebrin's inhibitory effect on mDia2 formin in pyrene florescence assays varied from preparation to preparation. We first tested and eliminated some of the trivial factors that may affect drebrin's activity – reducing conditions (we increased DTT concentration), the presence of detergents (IGEPAL CA 630), and pH (6.8-7.4). None of the above fully restored the activity of drebrin towards mDia2 formin in actin polymerization assays. Next, we hypothesized that the intrinsically disordered C-terminal region of drebrin (where one of mDia2 binding sites is located) may adopt different conformations due to variations in expression conditions or impurities, thereby masking the formin binding site. To test this directly we attempted partial denaturation and refolding of drebrin. This approach was justified because drebrin is known to be able to refold even after boiling [41]. For these experiments we incubated FL drebrin in semi-denaturing buffer (1M urea, 4.6mM Tris, pH 8, 89uM KCl, 0.89uM DTT) for 5min at 25^{o}C. Then, FL drebrin was dialyzed overnight into drebrin dialysis buffer (DDB: 5mM TRIS pH8, 100mM KCl; 1mM DTT) to refold. After dialysis, protein aggregates were removed by high-speed centrifugation (TLA100, 85,000 rpm, 20 min, 4^{o}C). Drebrin concentration was re-measured spectrophotometrically (ε_{278}=0.625, with a baseline at 360nm). The results presented in Fig.16 indicate that partial denaturation and refolding of drebrin A restores its activity towards mDia2

formin. We hypothesize that increased temperature during drebrin expression may affect its conformation. We are currently working to resolve this complication.

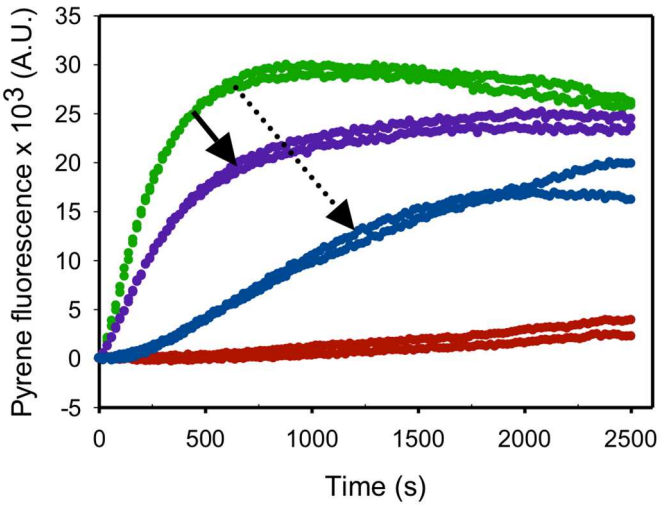

FIGURE 16: **Partial denaturation and refolding of full length drebrin A restores its inhibitory effect on actin polymerization driven by mDia2-FFC.**

Several full length drebrin preperations had significantly weaker inhibitory effect on mDia2-driven actin polymerization than other preperations tested in this study. We found that drebrin's effect on mDia2 activity can be recovered through drebrin's partial denaturation (1M urea) and refolding. Refolded full length drebrin (0.7uM, blue trace) inhibits mDia2 activity (dotted arrow) to a much greater extent than untreated full length drebrin(0.75uM, purple trace, solid arrow). [Green trace: mDia2-FFC mediated actin polymerization; Red trace: actin alone.] Two replicates per sample are shown.

Conditions: [Actin]=1uM (10% pyrene-maleimide), [mDia2-FFC]=30nM. Buffer: KMEH7.

References

1. Tønnesen, J., and Nägerl, U. V. (2016). Dendritic spines as tunable regulators of synaptic signals. Frontiers in psychiatry *7*, 101.
2. Lippman, J., and Dunaevsky, A. (2005). Dendritic spine morphogenesis and plasticity. J Neurobiol *64*, 47–57.
3. Robinson, C. M., Patel, M. R., and Webb, D. J. (2016). Super resolution microscopy is poised to reveal new insights into the formation and maturation of dendritic spines. [version 1; referees: 2 approved]. F1000Res *5*.
4. Hering, H., and Sheng, M. (2001). Dendritic spines: structure, dynamics and regulation. Nat Rev Neurosci *2*, 880–888.
5. Rudy, J. W. (2015). Actin dynamics and the evolution of the memory trace. Brain Res *1621*, 17–28.
6. Koganezawa, N., Hanamura, K., Sekino, Y., and Shirao, T. (2017). The role of drebrin in dendritic spines. Mol Cell Neurosci.
7. Korobova, F., and Svitkina, T. (2010). Molecular architecture of synaptic actin cytoskeleton in hippocampal neurons reveals a mechanism of dendritic spine morphogenesis. Mol Biol Cell *21*, 165–176.
8. Halpain, S. (2000). Actin and the agile spine: how and why do dendritic spines dance? Trends Neurosci *23*, 141–146.
9. Chazeau, A., and Giannone, G. (2016). Organization and dynamics of the actin cytoskeleton during dendritic spine morphological remodeling. Cell Mol Life Sci *73*, 3053–3073.
10. Soria Fregozo, C., and Pérez Vega, M. I. (2012). Actin-binding proteins and signalling pathways associated with the formation and maintenance of dendritic spines. Neurologia *27*, 421–431.

11. Shirao, T., Hanamura, K., Koganezawa, N., Ishizuka, Y., Yamazaki, H., and Sekino, Y. (2017). The role of drebrin in neurons. J Neurochem.
12. Ma, L., Li, Y., and Wang, R. (2015). Drebrin and cognitive impairment. Clin Chim Acta *451*, 121–124.
13. Shirao, T., and González-Billault, C. (2013). Actin filaments and microtubules in dendritic spines. J Neurochem *126*, 155–164.
14. Shim, K. S., and Lubec, G. (2002). Drebrin, a dendritic spine protein, is manifold decreased in brains of patients with Alzheimer's disease and Down syndrome. Neurosci Lett *324*, 209–212.
15. Ferhat, L. (2012). Potential role of drebrin a, an f-actin binding protein, in reactive synaptic plasticity after pilocarpine-induced seizures: functional implications in epilepsy. Int J Cell Biol *2012*, 474351.
16. Jin, M., Tanaka, S., Sekino, Y., Ren, Y., Yamazaki, H., Kawai-Hirai, R., Kojima, N., and Shirao, T. (2002). A novel, brain-specific mouse drebrin: cDNA cloning, chromosomal mapping, genomic structure, expression, and functional characterization. Genomics *79*, 686–692.
17. Mikati, M. A., Grintsevich, E. E., and Reisler, E. (2013). Drebrin-induced stabilization of actin filaments. J Biol Chem *288*, 19926–19938.
18. Kobayashi, C., Aoki, C., Kojima, N., Yamazaki, H., and Shirao, T. (2007). Drebrin a content correlates with spine head size in the adult mouse cerebral cortex. J Comp Neurol *503*, 618–626.
19. Chesarone, M. A., DuPage, A. G., and Goode, B. L. (2010). Unleashing formins to remodel the actin and microtubule cytoskeletons. Nat Rev Mol Cell Biol *11*, 62–74.
20. Hotulainen, P., Llano, O., Smirnov, S., Tanhuanpää, K., Faix, J., Rivera, C., and Lappalainen, P. (2009). Defining mechanisms of actin polymerization and depolymerization during dendritic spine morphogenesis. J Cell Biol *185*, 323–339.

21. Chazeau, A., Mehidi, A., Nair, D., Gautier, J. J., Leduc, C., Chamma, I., Kage, F., Kechkar, A., Thoumine, O., Rottner, K., et al. (2014). Nanoscale segregation of actin nucleation and elongation factors determines dendritic spine protrusion. EMBO J *33*, 2745–2764.
22. Miyagi, Y., Yamashita, T., Fukaya, M., Sonoda, T., Okuno, T., Yamada, K., Watanabe, M., Nagashima, Y., Aoki, I., Okuda, K., et al. (2002). Delphilin: a novel PDZ and formin homology domain-containing protein that synaptically colocalizes and interacts with glutamate receptor delta 2 subunit. J Neurosci *22*, 803–814.
23. Almuqbil, M., Hamdan, F. F., Mathonnet, G., Rosenblatt, B., and Srour, M. (2013). De novo deletion of FMN2 in a girl with mild non-syndromic intellectual disability. Eur J Med Genet *56*, 686–688.
24. Pellegrin, S., and Mellor, H. (2005). The Rho family GTPase Rif induces filopodia through mDia2. Curr Biol *15*, 129–133.
25. Schirenbeck, A., Bretschneider, T., Arasada, R., Schleicher, M., and Faix, J. (2005). The Diaphanous-related formin dDia2 is required for the formation and maintenance of filopodia. Nat Cell Biol *7*, 619–625.
26. Vizcarra, C. L., Bor, B., and Quinlan, M. E. (2014). The role of formin tails in actin nucleation, processive elongation, and filament bundling. J Biol Chem *289*, 30602–30613.
27. Gaillard, J., Ramabhadran, V., Neumanne, E., Gurel, P., Blanchoin, L., Vantard, M., and Higgs, H. N. (2011). Differential interactions of the formins INF2, mDia1, and mDia2 with microtubules. Mol Biol Cell *22*, 4575–4587.
28. Quinlan, M. E., Hilgert, S., Bedrossian, A., Mullins, R. D., and Kerkhoff, E. (2007). Regulatory interactions between two actin nucleators, Spire and Cappuccino. J Cell Biol *179*, 117–128.
29. Pechlivanis, M., Samol, A., and Kerkhoff, E. (2009). Identification of a short Spir interaction sequence at the C-terminal end of formin subgroup proteins. J Biol Chem *284*, 25324–25333.

30. Grintsevich, E. E., Galkin, V. E., Orlova, A., Ytterberg, A. J., Mikati, M. M., Kudryashov, D. S., Loo, J. A., Egelman, E. H., and Reisler, E. (2010). Mapping of drebrin binding site on F-actin. J Mol Biol *398*, 542–554.
31. Sharma, S., Grintsevich, E. E., Phillips, M. L., Reisler, E., and Gimzewski, J. K. (2011). Atomic force microscopy reveals drebrin induced remodeling of f-actin with subnanometer resolution. Nano Lett *11*, 825–827.
32. Gould, C. J., Maiti, S., Michelot, A., Graziano, B. R., Blanchoin, L., and Goode, B. L. (2011). The formin DAD domain plays dual roles in autoinhibition and actin nucleation. Curr Biol *21*, 384–390.
33. Harris, E. S., Rouiller, I., Hanein, D., and Higgs, H. N. (2006). Mechanistic differences in actin bundling activity of two mammalian formins, FRL1 and mDia2. J Biol Chem *281*, 14383–14392.
34. Worth, D. C., Daly, C. N., Geraldo, S., Oozeer, F., and Gordon-Weeks, P. R. (2013). Drebrin contains a cryptic F-actin-bundling activity regulated by Cdk5 phosphorylation. J Cell Biol *202*, 793–806.
35. Wegner, A. M., Nebhan, C. A., Hu, L., Majumdar, D., Meier, K. M., Weaver, A. M., and Webb, D. J. (2008). N-wasp and the arp2/3 complex are critical regulators of actin in the development of dendritic spines and synapses. J Biol Chem *283*, 15912–15920.
36. Spudich, J. A., and Watt, S. (1971). The regulation of rabbit skeletal muscle contraction. I. Biochemical studies of the interaction of the tropomyosin-troponin complex with actin and the proteolytic fragments of myosin. J Biol Chem *246*, 4866–4871.
37. Kaiser, D. A., Goldschmidt-Clermont, P. J., Levine, B. A., and Pollard, T. D. (1989). Characterization of renatured profilin purified by urea elution from poly-L-proline agarose columns. Cell Motil Cytoskeleton *14*, 251–262.
38. Li, F., and Higgs, H. N. (2003). The mouse Formin mDia1 is a potent actin nucleation factor regulated by autoinhibition. Curr Biol *13*, 1335–1340.

39. Grintsevich, E. E., Yesilyurt, H. G., Rich, S. K., Hung, R. J., Terman, J. R., and Reisler, E. (2016). F-actin dismantling through a redox-driven synergy between Mical and cofilin. Nat Cell Biol *18*, 876–885.

40. Gurel, P. S., Ge, P., Grintsevich, E. E., Shu, R., Blanchoin, L., Zhou, Z. H., Reisler, E., and Higgs, H. N. (2014). INF2-mediated severing through actin filament encirclement and disruption. Curr Biol *24*, 156–164.

41. Ishikawa, R., Hayashi, K., Shirao, T., Xue, Y., Takagi, T., Sasaki, Y., and Kohama, K. (1994). Drebrin, a development-associated brain protein from rat embryo, causes the dissociation of tropomyosin from actin filaments. J Biol Chem *269*, 29928–29933.